Available online at www.sciencedirect.com
ScienceDirect
Journal of the European Ceramic Society 31 (2011) 2535–2542
www.elsevier.com/locate/jeurceramsoc

Flow behavior of polymerizable ceramic suspensions as function of ceramic volume fraction and temperature

V. Tomeckova, J.W. Halloran *

University of Michigan, Department of Materials Science and Engineering, 2300 Hayward Street, Ann Arbor, MI 48109, USA

Available online 16 February 2011

Abstract

The effect of volume fraction and temperature on flow behavior is reported for suspensions of coarse silica powders in two non-aqueous polymerizable solutions. The concentration dependence of the viscosity at temperatures 25–75 °C can be reduced to a single Krieger–Dougherty curve for all suspensions. The temperature dependence of viscosity for suspensions with 60 vol% silica could be fit to an Arrhenius equation. The suspensions had a larger apparent activation energy than the suspension medium. This could be explained in terms of thermal dilution, where the higher thermal expansion of the liquid reduces the solids loading for very concentrated suspensions.

Keywords: D. SiO_2; Rheology; Suspensions

1. Introduction

Polymerizable ceramic suspensions have been extensively used for gel casting, where the suspension medium is gelled to solidify the green body, typically by heating the suspension to thermally initiate the polymerization reaction. Similar suspensions can be gelled with photoinitiation for applications such as tape casting,[1] ceramic stereolithography,[2–4] dental composites[5] and others. Typically gel casting suspensions are concentrated, with the volume fraction solids around 60 vol%, and tend to be quite viscous. The flow parameter that is important in practice is the suspension viscosity η_{susp}. The suspension viscosity is the product of the relative viscosity η_r, which includes the influence of the suspended solids and the colloidal effects, and the viscosity of the suspension medium η_o itself. Certain monomers can have a rather large viscosity. The viscosity of the monomers in this study ranges from 9 mPa s for 1,6-hexanediol diacrylate to 130 mPa s for ethoxylated (9) trimethylpropanone triacrylate, which can lead to inconveniently viscous suspensions.

Two approaches can reduce the suspension viscosity. Interparticle forces can be manipulated,[6–8] to decrease the relative viscosity η_r, which can be reduced down to its hydrodynamic minimum, which is often modeled with the Krieger–Dougherty expression. Anther way improve the fluidity of the suspension is to reduce the suspension medium viscosity η_o, which can be done by raising the temperature, or by replacing some of the more viscous monomers with less viscous "diluents".

The aim of this paper is to examine the flow behavior of a relatively coarse refractory silica powder suspended in two non-aqueous monomer solutions. These suspensions are dominated by hydrodynamic factors, since the combination of low powder surface area and small Hamaker constant make colloidal attractive forces minor. We show that the viscosity as a function of solid loadings for suspensions in several monomer solutions can be described in with the Krieger–Dougherty equation. The temperature dependence of the suspension viscosity $\eta_{susp}(T)$ was found to be larger then the temperature dependence of the suspension medium viscosity $\eta_o(T)$ due to a "thermal dilution" of the suspension as the liquid medium expands more than the solids. This paper concerns the combination of this thermal dilution effect to describe the flow behavior of a wide range of suspensions as a single Krieger–Dougherty expression in terms of a temperature-adjusted volume fraction.

2. Experimental

The UV curable monomers in this study were two non-water dispersible acrylate monomers 1,6 hexanediol diacrylate and polypropylene glycol (400) dimethacrylate, both received from Sartomer, USA. The diacrylate is bifunctional monomer that

* Corresponding author. Tel.: +1 734 763 1051; fax: +1 734 763 4788.
E-mail address: peterjon@umich.edu (J.W. Halloran).

0955-2219/$ – see front matter © 2011 Elsevier Ltd. All rights reserved.
doi:10.1016/j.jeurceramsoc.2011.01.019

Table 1
Some physical properties of monomers and diluents.

	Functionality	Viscosity (mPa s)	Density (g cm^{-3})	Molecular weight (g mol^{-1})	Theoretical polym. shrinkage (vol%)
Diacrylate	2	9	1.020	226	22.7
Glycol dimethacrylate	2	30	1.002	536	8.6
Triacrylate	3	130	1.110	692	11.5
Monoacrylate	1	8	0.980	208	11.2
Inert diluent	–	2–3	0.896	138	0

has a low viscosity 9 mPa s at 25 °C, but has a high polymerization shrinkage. The bifunctional glycol dimethacrylate has a higher viscosity 30 mPa s at 25 °C, but a lower polymerization shrinkage. To improve cross-linking, a trifunctional monomer ethoxylated (9) trimethylpropanone triacrylate (Sartomer, USA) was added to the diacrylate composition at the weight ratio 7/3, 5/5 and 3/7. This monomer has a high viscosity, 130 mPa s at 25 °C, has fast curing kinetics, and is a low skin irritation monomer.

A non-reactive solvent, decahydronaphthalene, cis + trans, 97% (also known as decalin) was used as an inert diluent to reduce viscosity. Decahydronaphthalene, $C_{10}H_{18}$ (Alfa Aesar) is a bicyclic organic compound widely used as a solvent in many industrial resins. Decalin does not participate in the polymerization reaction. A lower viscosity monomer was used as a reactive diluent. We used isobornyl acrylate (Sartomer, USA), which is a monofunctional acrylate monomer and has viscosity around 10 mPa s. Monomers and diluents were used at the weight ratio 7/3. Higher dilution would be desirable with respect to viscosity reduction, however, highly diluted systems do not exhibit good mechanical properties upon polymerization. Diluents were used also in case of low viscosity diacrylate suspensions since they reduce the polymerization shrinkage of the monomer. Some physical properties of the monomers and diluents are summarized in Table 1, showing the room temperature viscosity, the density and the theoretical polymerization shrinkage based on the difference in the density of the polymer and the monomer. At room temperature, all these monomer solutions are Newtonian in this range of shear rates. Table 2 shows the measured viscosities of the monomer mixtures, and the theoretical polymerization shrinkages inferred from a rule-of-mixtures.

The suspension formulations included a UV photoinitiator Irgacure 184 (Ciba, USA), which is 1-hydroxy-cyclohexyl-phenyl-ketone. Irgacure 184 has density 1.1–1.2 g cm^{-3} and was added at 2% with respect to monomer mass. The ceramic powder was a polydispersed silicon dioxide, 99.8%, metal basis (Alfa Aesar) with $d_{10} = 2.3$ μm, median size $d_{50} = 7$ μm, $d_{90} = 24.7$ μm, a specific area of 5 m^2/g and density of 2.2 g cm^{-3} (all from the manufacturer's specifications). This powder is a pulverized fused silica, with irregular particle shape. The powder was used as received without further purification. To produce a stable ceramic suspension Variquat CC-59 (Evonik, Degussa, Essen DE) was used as a dispersant in all systems in the amount of 3% with respect to the ceramic powder mass, which was found to be an optimum in all suspensions. Variquat CC-59 is alkoxylated ammonium phosphate of pH 7.5–9.5, density 1.04 g cm^{-3} and viscosity 3 Pa s at 20 °C (all from manufacturer's specifications).

Ceramic suspensions were prepared by the process of ball milling at room temperature. First, alumina milling media (6.35 mm diameter) were added into a polyethylene bottle (250 ml) in the amount corresponding to ∼1/15 of the bottle volume in order to prepare the suspensions under mixing conditions. The total amount of a suspension was calculated so that it fills half of the bottle volume. Monomers and dispersant were added first and ball milled at 30 rpm for ∼15 min to produce a well blended system. Ceramic powder was added incrementally—one-fourth at a time followed by the process of ball milling at 30 rpm for at least 3 h. After the last addition of the powder, the suspension was ball milled for ∼24 h (diacrylate suspensions) or at least 2–3 days in case of the more viscous glycol dimethacrylate and diacrylate/triacrylate suspensions. Then, photoinitiator was added and suspensions were ball milled for additional 6 h. The suspensions were degassed prior to the experiment.

The flow behavior of ceramic suspensions was measured on a cone-plate rheometer AR1000 (TA Instruments, New Castle DE, USA). The cone geometry had a diameter of 40 mm and angle 1.59°, with a 44 μm gap between the cone and the lower plate. The rheometer is equipped with a temperature controlled heating plate. Experiments were performed as a function of shear rate (1–100 s^{-1}) at ambient temperature 25 ± 1 °C and as a function of temperature (25–75 °C) at constant shear rate 45 s^{-1}. Temperature behavior of compositions with the inert diluent decalin

Table 2
Viscosity and theoretical polymerization shrinkage of the monomer solutions.

Monomer solution	Viscosity at 25 °C (mPa s)	Theoretical polym. shrinkage (vol%)
Diacrylate	7	22.7
Diacrylate/reactive diluent (7/3)	7	19.9
Diacrylate/inert diluent (7/3)	4	15.3
Glycol dimethacrylate	33	8.6
Glycol dimethacrylate/reactive diluent (7/3)	20	9.4
Glycol dimethacrylate/inert diluent (7/3)	10	6.0
Diacrylate/triacrylate (7/3)	14	19.3
Diacrylate/triacrylate (5/5)	23	17.1
Diacrylate/triacrylate (3/7)	48	14.8

Table 3
Power law parameters for suspension viscosity for 60% silica in different monomer media.

Monomer medium	K	n	Shear rate range
Diacrylate	0.66	1	1–100 s^{-1}
Diacrylate/reactive diluent (7/3)	0.66	1	1–100 s^{-1}
Diacrylate/inert diluent (7/3)	0.91 ± 0.14	0.64 ± 0.04	1–10 s^{-1}
	0.4	1	10–100 s^{-1}
Glycol dimethacrylate	1.57 ± 0.08	1.31 ± 0.03	10–100 s^{-1}
Glycol dimethacrylate/reactive diluent (7/3)	1.05 ± 0.27	1.25 ± 0.08	10–100 s^{-1}
Glycol dimethacrylate/inert diluent (7/3)	0.71 ± 0.11	1.23 ± 0.06	10–100 s^{-1}
Diacrylate/triacrylate (7/3)	0.88 ± 0.11	1.27 ± 0.07	10–100 s^{-1}
Diacrylate/triacrylate (5/5)	1.22 ± 0.20	1.29 ± 0.04	10–100 s^{-1}
Diacrylate/triacrylate (3/7)	2.20 ± 0.07	1.30 ± 0.03	10–100 s^{-1}

was studied in the temperature range 25–50 °C due to low flash point of decalin. A solvent trap was used in to minimize the evaporation during all measurements.

3. Results and discussion

Fig. 1 shows the viscosity curves for the diacrylate and glycol dimethacrylate suspensions with 60 vol% solid loadings, with and without diluents. The experiments were performed at 25 °C in the range of shear rates 1–100 s^{-1}. The glycol dimethacrylate suspensions are much more viscous than the diacrylate suspensions. For example, the viscosity of the glycol dimethacrylate suspension is above 5 Pa s at 45 s^{-1} while the diacrylate suspension has viscosity of ~0.7 Pa s at the same shear rate. This is a result of ~3 times higher viscosity of the glycol dimethacrylate medium compared to the diacrylate monomer, since viscosity of the loaded suspensions reflects the viscosity of the monomer.

The viscosity of the suspensions can be significantly reduced by diluents, since they reduce the viscosity of the monomer solution as shown in Table 2. For example, the viscosity of the glycol dimethacrylate suspension is reduced by the addition of the reactive diluent to ~2.7 Pa s (at 45 s^{-1}) and the inert diluent significantly decreased the viscosity to 1.7 Pa s (at 45 s^{-1}). When the reactive diluent was used in the diacrylate suspension, the viscosity of the suspension remained almost the same 0.70 ± 0.08 Pa s in this range of shear rates (1–100 s^{-1}), since the viscosities of the monomers are similar. On the other hand, the inert diluent decalin has viscosity ~3 times lower than the diacrylate monomer and decreased the overall viscosity of the diacrylate suspension.

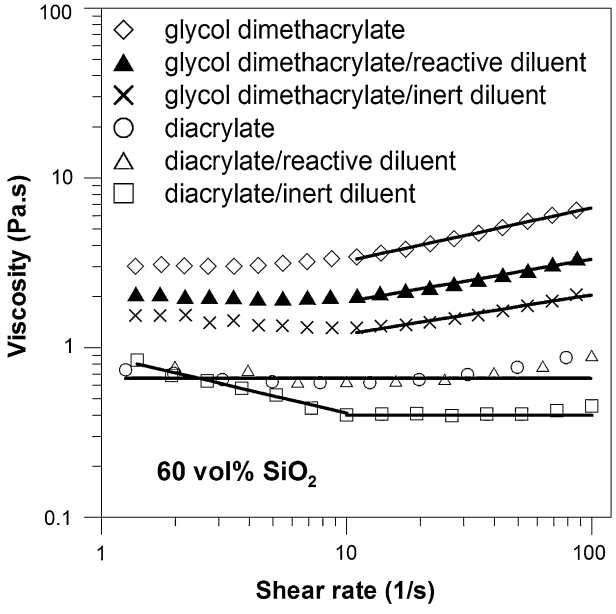

Fig. 1. Suspension viscosity vs. shear rate for 60 vol% silica in different monomer media. Monomers and diluents were used at the weight ratio 7/3. The symbols represent the measured data and the lines are the power law fit. The power law fitting paramters are summarized in Table 3.

There is a noticeable difference in the shear rate dependence for these suspensions. The diacrylate suspensions with no and with reactive diluent appear to be almost Newtonian and the diacrylate suspensions with inert diluent are slightly shear thinning at low shear rates (1–100 s^{-1}) and somewhat Newtonian at higher shear rates (10–100 s^{-1}). On the other hand, the glycol dimethacrylate suspensions are shear thickening at higher shear rates (10–100 s^{-1}) and somewhat Newtonian at lower shear rates (1–10 s^{-1}).

These flow curves could be fit with an expression for a power law fluid:

$$\eta_{\text{effective}} = K\gamma^{n-1} \quad (1)$$

where γ is shear rate, K is a consistency index and n exponent gives information about the suspension. Systems having $n = 1$ are Newtonian, $n > 1$ and $n < 1$ correspond to shear thickening and shear thinning behavior, respectively. Power law parameters for diacrylate and glycol dimethacrylate suspensions (60 vol%) with and without diluents are summarized in Table 3. The lines drawn through some of the data in Fig. 1 represent the power law fits. In the shear rate range 10–100 s^{-1}, the glycol dimethacrylate suspension has $n = 1.31$. The reactive and inert diluent decreased the n exponent to 1.24 ± 0.01. The diacrylate suspensions with and without the reactive diluent were nearly Newtonian and the viscosity was 0.70 ± 0.08 Pa s in the shear rate range 1–100 s^{-1}, and the data was satisfactory fitted with power law with $n = 1$. On the other hand, the inert diluent brought certain degree of pseudo-plasticity into diacrylate suspensions and at lower shear rates (1–10 s^{-1}) the suspension was slightly shear thinning and the n exponent was reduced to 0.64. At higher shear rates (10–100 s^{-1}), the diacrylate/inert diluent suspension was almost Newtonian.

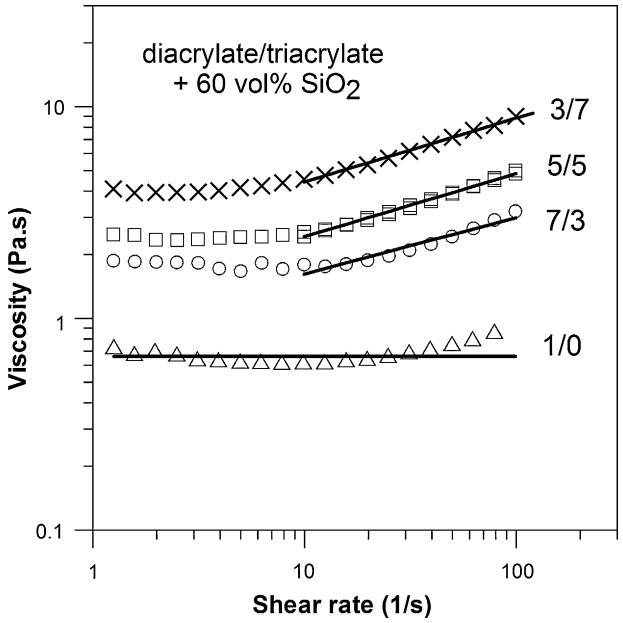

Fig. 2. Suspension viscosity vs. shear rate for 60 vol% silica in diacrylate/triacrylate. The symbols represent the measured data and the lines are the power law fit. The power law fitting paramters are summarized in Table 3.

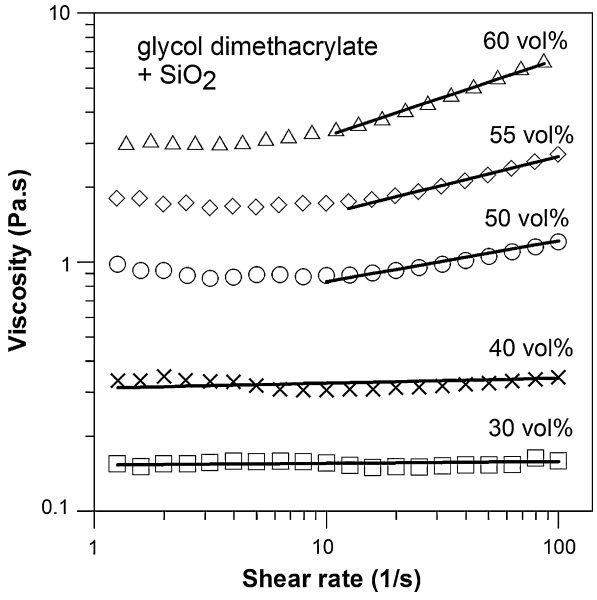

Fig. 3. Suspension viscosity vs. shear rate for different solids loading in glycol dimethacrylate.

Higher functionality monomers are added to photopolymerizable suspensions to improve cross-linking, however, higher viscosity of the triacrylate results in difference in rheological behavior when used at higher concentrations. Fig. 2 shows the suspension viscosity vs. shear rate for the diacrylate/triacrylate suspensions with 60 vol% SiO_2, at room temperature. Diacrylate/triacrylate monomer solutions were prepared at the weight ratio 7/3, 5/5 and 3/7. The more fluid diacrylate suspension is nearly Newtonian in this range of shear rate, but as the concentration of the more viscous triacrylate increases, the suspensions become more viscous. Similarly to glycol dimethacrylate suspensions, the diacrylate/triacrylate suspensions are almost Newtonian at lower shear rates (1–10 s^{-1}) and shear thickening at higher shear rates (10–100 s^{-1}). The power law fits are represented by the lines drawn through some of the data in Fig. 2. The flow exponent goes from $n \sim 1$ for the diacrylate suspension to $n \sim 1.3$ for the diacrylate/triacrylate (3/7) suspension. Power law parameters for diacrylate/triacrylate suspensions (60 vol%) are summarized in Table 3.

Further, the effect of ceramic volume content on the rheology behavior of the glycol dimethacrylate suspensions was investigated. Fig. 3 plots the suspension viscosity vs. shear rate for the glycol dimethacrylate suspensions with 30–60 vol% silica. The lines represent the power law fit. Suspensions with lower ceramic volume content (40 and 30 vol%) are almost Newtonian and were satisfactory fitted with power law curves with exponent $n = 1$. The 60, 55 and 50 vol% suspensions are almost Newtonian at lower shear rates (1–10 s^{-1}) and exhibit dilatancy at higher shear rates (10–100 s^{-1}). As the ceramic volume content increases from 50 to 60 vol%, also the exponent increases from $n \sim 1.16$ to $n \sim 1.31$. Power law model parameters are shown in Table 4.

Fig. 4 shows the apparent suspension viscosity at 45 s^{-1} as a function of ceramic volume fraction, for the glycol dimethacrylate suspensions with and without diluents. All compositions show a sharp rise in viscosity above 50 vol%. These suspension viscosity data appear to might have different Krieger–Dougherty limits. However, the diluent decreases the viscosity of the glycol dimethacrylate solutions. Thus, the data can be compared via reduced viscosity considering the viscosity of the suspension and the liquid media:

$$\eta_{\text{reduced}} = \frac{\eta_{\text{suspension}}}{\eta_{\text{medium}}} \tag{2}$$

Fig. 5 shows the reduced viscosity of the suspensions in glycol dimethacrylate solutions as a function of volume fraction ceramic, showing the data can be approximated by a single line. A modified Krieger–Dougherty (K–D) equation of the form[9]:

$$\eta_{\text{reduced}} = \left(1 - \frac{\beta\Phi}{\Phi_0}\right)^{-[\eta]\Phi_0} \tag{3}$$

was used to calculate the K–D parameters. In Eq. (3) β is effective packing factor of the powder, Φ is volume fraction of the ceramic powder, Φ_0 is theoretical packing factor for ceramic particles and $[\eta]$ is intrinsic viscosity of the suspension. These are polydispersed suspensions with a particle size distribution

Table 4
Power law parameters for suspension viscosity for glycol dimethacrylate suspension with varying ceramic volume content.

Solid loadings (vol%)	K	n	Shear rate range
30	0.15	1	1–100 s^{-1}
40	0.31	1	1–100 s^{-1}
50	0.57 ± 0.03	1.16 ± 0.04	10–100 s^{-1}
55	0.92 ± 0.20	1.23 ± 0.03	10–100 s^{-1}
60	1.57 ± 0.08	1.31 ± 0.06	10–100 s^{-1}

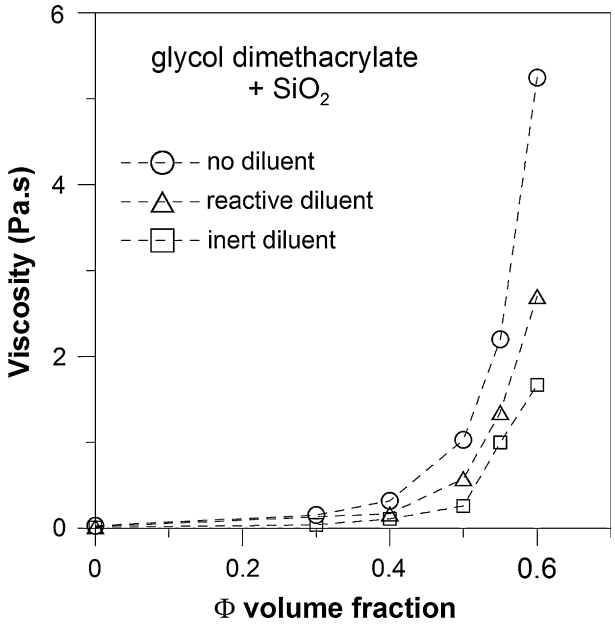

Fig. 4. Suspension viscosity at 45 s^{-1} for Fig. 3 data (glycol dimethacrylate with no diluent) and for glycol dimethacrylate with diluents. Monomers and diluents were used at the weight ratio 7/3.

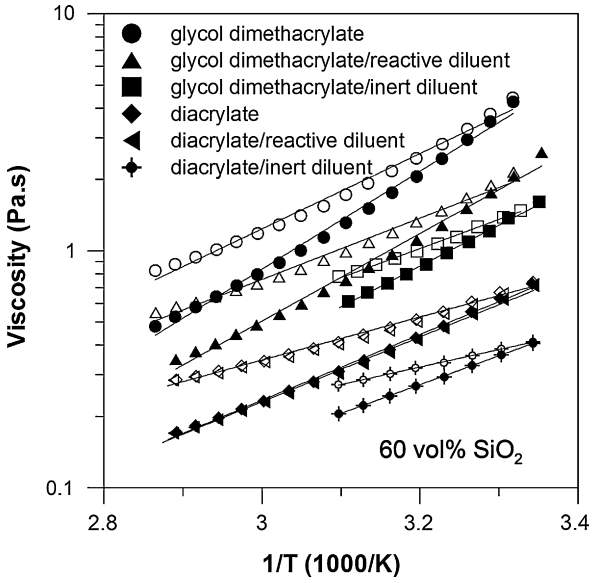

Fig. 6. Suspension viscosty vs. temperature. Monomers and diluents were used at the weight ratio 7/3. Closed symbols represent the measured data and open symbols represent the adjustment for thermal dilution. The lines represent Arrhenius fit.

from submicrons to hundreds of micrometers, but are treated as bimodal, packing factor for bimodal powders[9] with $\Phi_0 = 0.72$. Data for glycol dimethacrylate suspensions with and without diluent was fitted with the K–D model with $[\eta] = 2.5$ (appropriate for spherical particles[9]) and empirically determined $\beta = 1.16$. Notice that the K–D model only involves hydrodynamic flow of the liquid past rigid particles. Colloidal effects from interparticle attractive forces are not involved in the K–D model, so a fit to K–D behavior suggests that the silica-monomer suspensions are simple fluids with non-attracting particles. The β parameter has been often used to determine the layer thickness of absorbed dispersant.[6–9] This approach, however, is not appropriate for this powder with a very broad particle distribution.

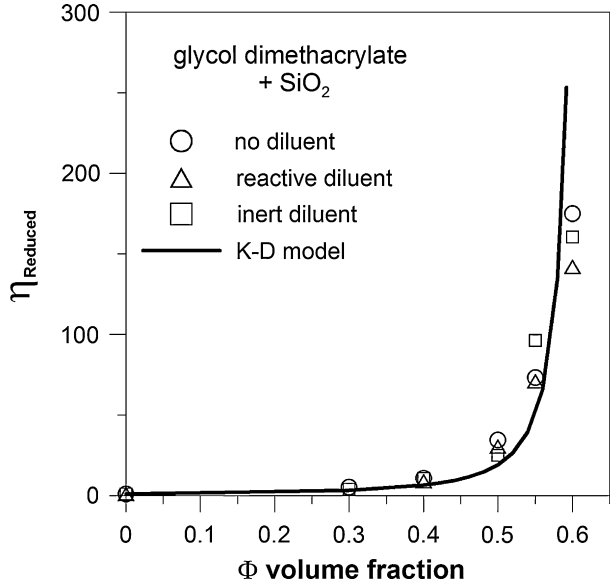

Fig. 5. Reduced viscosity vs. ceramic volume fraction for Fig. 4 data. All data can be fitted with a single K–D curve.

4. Temperature dependence

The temperature dependence of the suspension apparent viscosity $\eta_{suspension}(T)$ at 45 s^{-1} for the diacrylate and glycol dimethacrylate 60 vol% silica suspensions, with and without diluents, appears in Fig. 6 (closed symbols). The viscosity–temperature data for the diacrylate/triacrylate suspensions with nominally 60 vol% silica is shown in Fig. 7 (closed symbols) for diacrylate/triacrylate weight ratios of 3/7, 5/5, 7/3, and 1/0 (i.e. only diacrylate). Both Figs. 6 and 7 are fitted well by the Arrhenius equation. The apparent activation energies for these suspensions are also summarized in Table 5.

To understand the temperature dependence of the viscosity of powder suspensions $\eta_{suspension}(T)$ from Eq. (2), the behavior of the monomer solutions $\eta_{medium}(T)$ has to be known. The apparent viscosities of all the monomer solutions at 45 s^{-1} are presented in Fig. 8. Error bars are not shown for clarity, but the variation in these η_{medium} data is smaller than ±5%. The logarithm of the viscosity is plotted against the inverse of temperature, and is fit well by an Arrhenius relation. The apparent activation energies for the η_{medium} are listed in Table 5. For example, the activation energies of the diacrylate and glycol dimethacrylate monomer were on the order of ~18 and 28 kJ/mol, respectively.

Notice that the apparent activation energy for viscosity for the suspensions $\eta_{suspension}$ is on average ~25–30% higher than the activation energy for monomer solutions η_{medium}. This anomaly can be resolved by considering the *thermal dilution* of the suspensions. The ceramic volume content changes with temperature because of thermal expansion of the liquid. At increased tem-

Table 5
Activation energies from Arrhenius relation for suspension medium and 60 vol% silica suspensions.

Monomer solution	Suspension medium Apparent activation energy (kJ/mol)	60 vol% silica suspensions nominal Apparent activation energy (kJ/mol)	Thermally diluted 60 vol% silica suspensions Activation energy determined from viscosity corrected for thermal dilution (kJ/mol)
Diacrylate	18.3 ± 0.2	26.5 ± 0.3	17.4 ± 0.2
Diacrylate/reactive diluent (7/3)	19.0 ± 0.2	26.2 ± 0.3	17.0 ± 0.2
Diacrylate/inert diluent (7/3)	16.8 ± 0.2	23.3 ± 0.3	14.1 ± 0.2
Glycol dimethacrylate	27.6 ± 0.4	39.5 ± 0.5	30.4 ± 0.4
Glycol dimethacrylate/reactive diluent (7/3)	25.1 ± 0.3	33.8 ± 0.4	24.8 ± 0.3
Glycol dimethacrylate/inert diluent (7/3)	20.3 ± 0.9	33.0 ± 0.4	23.9 ± 0.3
Diacrylate/triacrylate (7/3)	22.8 ± 0.3	33.4 ± 1.0	23.8 ± 0.3
Diacrylate/triacrylate (5/5)	25.4 ± 0.3	36.9 ± 1.1	27.3 ± 0.3
Diacrylate/triacrylate (3/7)	29.5 ± 0.4	41.1 ± 1.4	31.3 ± 0.4

peratures, thermal expansion of the monomer results in *thermal dilution* of the volume fraction:

$$\Phi(T) = \frac{V_S}{V_S + V_L} = \frac{V_S}{V_S + V_L(25) + V_L(25)\,\alpha(T-25)} \quad (4)$$

where α is the volumetric thermal expansion coefficient for the monomer, V_S is volume of the solid and V_L is volume of the liquid. Chu and Halloran determined the α for similar acrylate monomers to be 6×10^{-4}/°C.[9] Therefore, the actual volume fraction for a suspension with ceramic volume fraction $\Phi = 0.6000$ at 25 °C, Φ decreases to 0.5929 at 75 °C. This appears to be a small difference, but viscosity is very sensitive to volume fraction at these high concentrations as will be discussed below. The volumetric thermal expansion of the liquid medium is about 6×10^{-4}/°C, while of the silica particles is much lower, on order 10^{-7}/°C. This can cause a small decrease in volume fraction solids by the thermal dilution effect.[10] Table 6 shows the actual volume fraction of the nominally 60.0 vol% suspension at temperatures up to 75 °C.

Table 6
Krieger–Dougherty thermal dilution correction for liquids with thermal expansion coefficient of 0.0006/°C.

Temperature (°C)	Volume fraction ceramic corrected for thermal dilution	K–D thermal dilution factor (Eq. (5))
25	0.6000	1.0000
35	0.5986	0.8862
45	0.5971	0.7917
55	0.5957	0.7124
65	0.5943	0.6451
75	0.5929	0.5874

Fig. 9 shows the suspension viscosity at 45 s^{-1} for diacrylate/triacrylate (3/7) suspensions at three temperatures, plotted against *nominal* ceramic volume fraction at the room temperature. There are three distinct curves, with different behavior

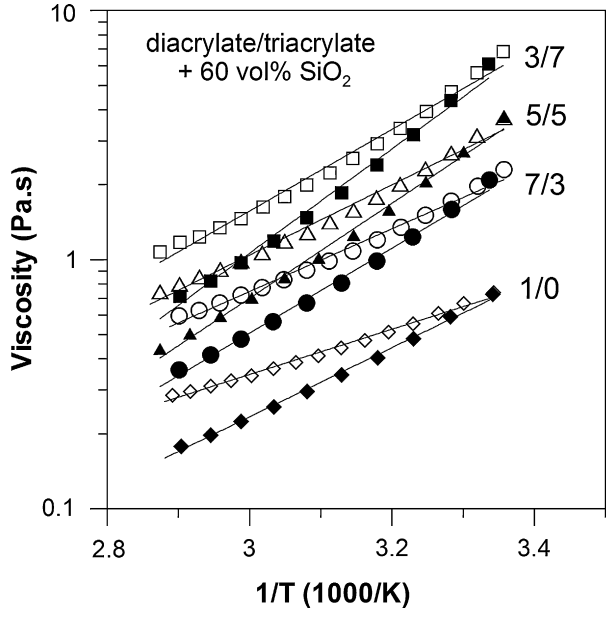

Fig. 7. Suspension viscosty vs. temperature. Closed symbols represent the measured data and open symbols represent the adjustment for thermal dilution. The lines represent Arrhenius fit.

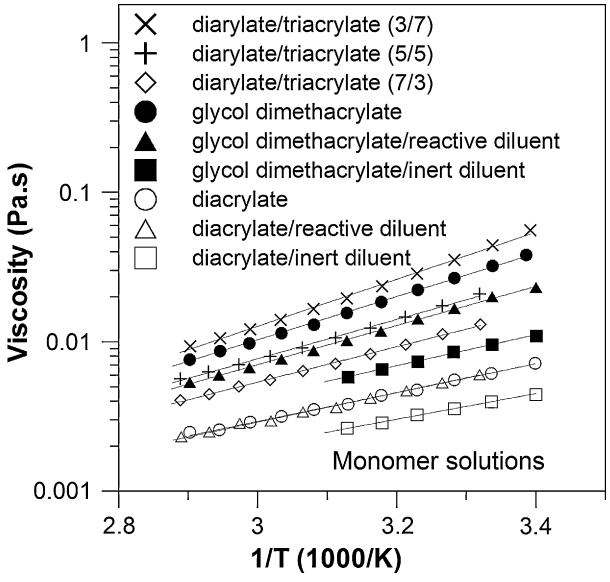

Fig. 8. Viscosity of monomer solutions vs. temperature. Monomers and diluents were used at the weight ratio 7/3. The lines represent Arrhenius fit.

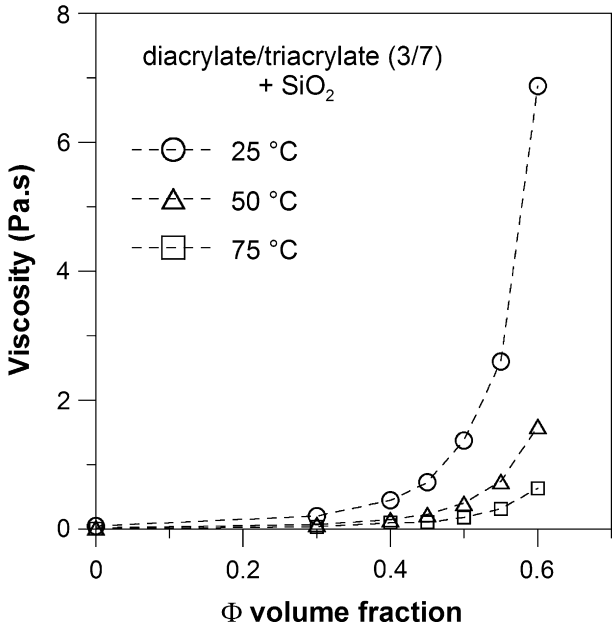

Fig. 9. Diacrylate/triacrylate (3/7) suspension viscosity at 45 s^{-1} vs. volume fraction at three temperatures.

for each temperature. The temperature dependence of the suspension viscosity includes both the temperature-dependent monomer viscosity (which can be removed through the reduced viscosity) and the volume fraction of ceramic, which is temperature dependent due to the thermal dilution effect. If these are the only factors, a K–D plot using both reduced viscosity and the temperature-corrected volume fraction should collapse all the data to the same curve as shown in Fig. 10. The β factor was determined to be 1.16 and maximum packing factor $\phi_0 = 0.72$.

Note that the reduced viscosities of the diacrylate/triacrylate suspensions at several temperatures (Fig. 10 data) and the

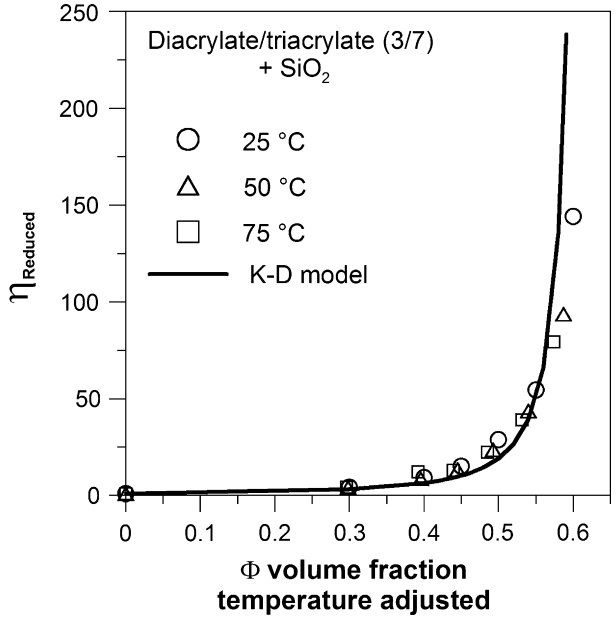

Fig. 10. Reduced viscosity vs. ceramic volume fraction for Fig. 9 data. All data can be fitted with a single K–D curve.

reduced viscosities of the glycol dimethacrylate suspensions with diluents (Fig. 5 data) can be all represented by a single K–D plot with β factor empirically determined to be 1.16 and maximum packing factor $\phi_0 = 0.72$. Chu and Halloran successfully used the K–D fit for alumina suspensions based on propoxylated neopentoglycol diacrylate/isobornyl acrylate mixture (the experiments were performed at 25, 45, 65 and 75 °C).[9] Chu determined the β factor 1.21 and maximum packing factor $\phi_0 = 0.64$. The maximum loading in case of the alumina suspensions was $\phi = 0.50$ while the silica suspensions in this study were prepared up to $\phi = 0.60$. The systems also differ in particle size. The alumina particles have diameter 0.4 μm and it is a monodisperse powder, while the silica particles are polydisperse with $d_{50} = 7$ μm. The K–D fitting in case of alumina suspension was determined for the high shear thinning region, while in case of silica the experiments were performed at 45 s^{-1} where the suspension is slightly shear thickening, so only approximate agreement is expected. Nevertheless, for the same particle size and same shear rate the suspensions fall into one single curve. It can be concluded that they behave similarly regardless of the monomer system and the experiment temperature, and the only variable seems to be the ceramic volume content.

The difference between the temperature dependence of viscosity for the suspension and monomer is unexpected, and larger apparently activation energy for viscous flow of the suspension (Table 5) is surprising. The temperature dependence of the *suspensions* should be the same as the temperature dependence of the liquid suspension *medium*, the monomer solution in this case. To explain this difference, consider again the small change in volume fraction from thermal dilution, which can be associated with a larger change of suspension viscosity for very concentrated suspension. This can be obtained with the K–D model given by Eq. (3). These can be combined to obtain K–D equation correction factor, I, that accounts for the thermal dilution effect as:

$$I = \left(1 - \frac{\beta \Phi_{\text{nom}}}{\Phi_0}\right)^{+[\eta]\Phi_0} \left(1 - \frac{\beta\, \Phi(T)}{\Phi_0}\right)^{-[\eta]\Phi_0} \tag{5}$$

where the K–D parameters are as previously defined, with Φ_{nom} being the nominal room temperature volume fraction solids and $\Phi(T)$ being the volume fraction corrected for thermal dilution at temperature T. For the $\Phi_{\text{nom}} = 0.60$, we obtain the thermal dilution I-factor for each temperature. The K–D thermal dilution factor appears in Table 6 along with data for corrected ceramic volume content. Then, an estimated "corrected" suspension viscosity is obtained by dividing each *measured* suspension viscosity by the I-factor for that temperature: $\eta_{\text{corrected}}(T) \sim \eta_{\text{suspension}}(T)/I(T)$.

The K–D temperature corrected temperature dependence curves are shown in Figs. 6 and 7 (open symbols). Notice that after correcting for thermal dilution the temperatures dependence of the suspension viscosity $\eta_{\text{corrected}}$ is somewhat smaller, as some of the excessive temperature dependence for the measured viscosity of the suspensions can be attributed to thermal dilution. The apparent activation energies for viscous flow of suspensions using the K–D thermal dilution-corrected viscosi-

ties are listed in Table 5. These are much closer to the activation energies for the monomer solutions η_{medium}. Thus most of the excess temperature dependence for viscous flow for these suspensions can be attributed to the monomer. Apparently, with the highly concentrated suspensions as are used in gel casting, one must consider both the temperature dependence of the viscosity itself and the effects of thermal dilution.

5. Conclusion

Viscosity of the suspensions varied with the viscosity of the monomer solution, as affected by temperature and diluents, and by the ceramics solids loading. The diluents viscosity and temperature effect could be removed by use of the reduced viscosity. The reduced viscosities of the suspensions could be described by a modified Krieger–Dougherty, with $\beta = 1.16$ and $\Phi_0 = 0.72$, for all the monomer solutions at room temperature. Satisfactory fit to the hydrodynamic Krieger–Dougherty model suggests that suspension rheology for this system is dominated by simple hydrodynamics.

Suspension viscosity at temperatures up to 75 °C can be described by the same Krieger–Dougherty parameters and collapse to a single curve, if the volume fraction is corrected for thermal dilution. For each suspension, the temperature dependence of viscosity can be fit with an Arrhenius Equation, but the apparent activation energy is larger than the activation energy for the monomer solutions. The excess temperature dependence can be attributed to thermal dilution. The effect of thermal dilution on the apparent activation energy for viscous flow of suspensions can be removed with a correction factor obtained from the Krieger–Dougherty parameters.

Acknowledgements

This research was supported by the United States Defense Advanced Research Projects Agency under Contract HR0011-07-1-0034, with Professor Suman Das of the Georgia Institute of Technology. The authors thank an anonymous reviewer for pointing out the Hamaker constant of silica in these media.

References

1. Chartier T, Hinczewski C, Corbel S. UV curable systems for tape casting. *Journal of the European Ceramic Society* 1999;**19**:67–74.
2. Hinczewski C, Corbel S, Chartier T. Ceramic suspensions suitable for stereolithography. *Journal of the European Ceramic Society* 1998;**18**:583–90.
3. Griffith ML, Halloran JW. Free form fabrication of ceramics via stereolithography. *Journal of the American Ceramic Society* 1996;**79**:2601–8.
4. Chu GT-M, Brady GA, Miao W, Halloran JW, Hollister SJ, Brei D. Ceramic SFF by Direct and Indirect Stereolithography. In: *Mat. Res. Soc. Symp. Proc., Vol. 542*. 1999.
5. Chung KH, Sharma B, Greener EH. Polymerization kinetics in dental acrylics. *Dental Materials* 1986;**2**:275–8.
6. Bergström L. Rheological properties of concentrated nonaqueous silicon nitride suspension. *Journal of the American Ceramic Society* 1996;**79**:3033–40.
7. Guiterrez AC, Moreno R. Interpartical potentials in non-aqueous silicon nitride suspensions. *Journal of the American Ceramic Society* 2003;**86**:59–64.
8. Ferreira JMF, Diz HMM. Effect of solids loading on slip-casting performance of silicon carbide slurries. *Journal of the American Ceramic Society* 1999;**82**:1993–2000.
9. Chu TMG, Halloran JW. High-temperature flow behavior of ceramic suspensions. *Journal of the American Ceramic Society* 2000;**83**(9):2189–95.
10. Hrdina KE, Halloran JW. Dimensional changes during binder removal in a mouldable ceramic system. *Journal of Materials Science* 1998;**33**:2805–15.